Efficient discovery of potently neutralizing SARS-CoV-2 antibodies using LIBRA-seq with ligand blocking

Andrea R. Shiakolas[1,2], Nicole Johnson[3], Kevin J. Kramer[1,2], Naveenchandra Suryadevara[1], Daniel Wrapp[3], Sivakumar Periasamy[4,6], Kelsey A. Pilewski[1,2], Nagarajan Raju[1,2], Rachel Nargi[1], Rachel E. Sutton[1], Lauren Walker[1,2], Ian Setliff[1], James E. Crowe Jr[1,2,7], Alexander Bukreyev[4,5,6], Robert H. Carnahan[1,7], Jason S. McLellan[3], Ivelin S. Georgiev[1,2,8,9,10,11,*]

[1]Vanderbilt Vaccine Center, Vanderbilt University Medical Center, Nashville, TN, 37232, USA

[2]Department of Pathology, Microbiology, and Immunology, Vanderbilt University Medical Center, Nashville, TN, 37232, USA

[3]Department of Molecular Biosciences, The University of Texas at Austin, Austin, TX, 78712, USA

[4]Department of Pathology, University of Texas Medical Branch at Galveston, Galveston TX 77555, USA

[5]Department of Microbiology and Immunology, University of Texas Medical Branch at Galveston, Galveston TX 77555, USA

[6]Galveston National Laboratory, University of Texas Medical Branch at Galveston, Galveston TX 77555, USA

[7]Department of Pediatrics, Vanderbilt University Medical Center, Nashville, TN, 37232, USA

[8]Vanderbilt Institute for Infection, Immunology, and Inflammation, Vanderbilt University Medical Center, Nashville, TN, 37232, USA

[9]Department of Electrical Engineering and Computer Science, Vanderbilt University, Nashville, TN, 37232, USA

[10]Center for Structural Biology, Vanderbilt University, Nashville, TN, 37232, USA

26 [11]Program in Computational Microbiology and Immunology, Vanderbilt University Medical

27 Center, Nashville, TN, 37232, USA

28 *Corresponding author: ivelin.georgiev@vanderbilt.edu

29

30

31

32

33

ABSTRACT

SARS-CoV-2 therapeutic antibody discovery efforts have met with notable success but have been associated with a generally inefficient process, requiring the production and characterization of exceptionally large numbers of candidates for the identification of a small set of leads. Here, we show that incorporating antibody–ligand blocking as part of LIBRA-seq, the high-throughput sequencing platform for antibody discovery, results in efficient identification of ultra-potent neutralizing antibodies against SARS-CoV-2. LIBRA-seq with ligand blocking is a general platform for functional antibody discovery targeting the disruption of antigen–ligand interactions.

45 Technologies for developing preventive and therapeutic measures that can counteract
46 potential pandemics are of utmost significance for public health. The ongoing COVID-19
47 pandemic, for example, has emphasized the importance of developing effective
48 countermeasures quickly. Through various pandemic preparedness initiatives, effective SARS-
49 CoV-2-neutralizing antibodies were discovered and validated within months[1-7], as were SARS-
50 CoV-2 vaccine candidates[8]. However, even with such unprecedented speed of vaccine and
51 therapeutic development, the pandemic has inflicted devastating worldwide effects, including
52 the loss of millions of human lives, a long-lasting burden on the healthcare system, and
53 economic turmoil. Accelerating actions by several weeks or months can make an enormous
54 difference in an exponentially evolving pandemic, especially at the early stages of infection
55 spread. Therefore, the efficient discovery of effective countermeasures against emerging
56 pathogens can play a critical role in pandemic preparedness for future infectious disease
57 outbreaks.
58 Antibodies are a major modality for therapy against a wide range of diseases, including
59 infectious diseases, cancer, autoimmunity, cardiovascular, hematologic, neurologic diseases,
60 and others. Antibody discovery efforts have relied on a broad range of technologies, such as
61 hybridoma generation, antigen-specific B cell sorting, phage or yeast display, single-cell B cell
62 sequencing and others[9-14]. Overall, these efforts aim to identify paired heavy–light chain
63 antibody sequences isolated from human or animal samples with prior antigen exposure,
64 followed by monoclonal antibody production and functional characterization. However, with
65 these approaches for antibody discovery, limited information is typically obtained about the
66 antigen specificity of antibody candidates at the screening step. The recent development of the
67 LIBRA-seq (linking B cell receptor to antigen specificity through sequencing) technology enables
68 the simultaneous mapping of antibody sequence to antigen specificity for a large number of
69 antigens in a single next-generation sequencing experiment[15]. LIBRA-seq uses DNA-barcoded
70 antigens to transform B cell receptor (BCR)-antigen binding into a sequence-able event and is

71 of unique utility for discovering broadly reactive antibodies for pathogens that exhibit substantial
72 antigen variability. LIBRA-seq has been applied successfully to identify broadly reactive
73 antibodies against HIV-1, influenza viruses, and coronaviruses[15, 16].
74 Although using antigen binding alone as a readout can result in the successful
75 identification of functional antibodies, the discovery process can be inefficient, requiring time-
76 intensive subsequent monoclonal antibody validation steps. This limitation was exemplified by
77 the SARS-CoV-2 antibody discovery initiatives over the past year. Although these efforts have
78 met with notable success, resulting in numerous antibodies and antibody cocktails in clinical
79 trials or approved for emergency use[17-19], testing of large numbers of antibodies (frequently
80 hundreds to thousands) was generally required. Typically, a small fraction of tested antibodies
81 was neutralizing, with hit rates in the range of 0.3 to 23% in various studies[2-7].
82 To overcome this limitation, we developed LIBRA-seq with ligand blocking, a second-
83 generation LIBRA-seq technology that incorporates a functional readout into the antibody
84 discovery process. To achieve this goal, a ligand and its cognate target antigen(s) are each
85 labeled with a unique oligonucleotide barcode (**Supplementary Figure 1A**), enabling the
86 transformation of antigen-ligand interactions into sequence-able events. This allows for the
87 identification of B cells that have high LIBRA-seq scores for the target antigen(s) and low
88 LIBRA-seq scores for the ligand, as B cells that are likely able to potently block antigen-ligand
89 interactions (**Supplementary Figure 1A**). Therefore, a single high-throughput LIBRA-seq with
90 ligand blocking experiment provides both binding (antigen recognition) and functional (ligand
91 blocking) information for thousands of B cells at a time, at the single-cell level.
92 As a proof of concept, we performed antibody discovery for SARS-CoV-2-specific
93 antibodies from the peripheral B cells from convalescent subjects with past SARS-CoV-2
94 infection. This provides a suitable opportunity for validating the LIBRA-seq with ligand blocking
95 technology since antibodies that block the interactions of the SARS-CoV-2 spike (S) protein with
96 its receptor angiotensin-converting enzyme 2 (ACE2) are among the most potently neutralizing

97 identified to date[2-7, 17-19]. We performed three separate LIBRA-seq experiments, with screening
98 libraries that included: experiment 1, ACE2 and SARS-CoV-2 S; experiment 2, a titration series
99 of different aliquots of SARS-CoV-2 S, each labeled with a unique barcode; and experiment 3,
100 ACE2 and a titration series of S (**Figure 1A**). The incorporation of a titration series of the S
101 antigen in the LIBRA-seq screening library for experiments 2 and 3 aimed to assess the
102 strength of BCR-antigen interactions through a sequencing readout (**Supplementary Figure**
103 **1B, C**). The antigen screening library for each of the experiments also included an influenza
104 virus hemagglutinin and an HIV-1 envelope variant protein as controls.

105 The application of LIBRA-seq resulted in 829, 830, and 957 antigen-specific B cells for
106 the three experiments, respectively. We prioritized a set of B cells for monoclonal antibody
107 production and validation based on the following conditions: for experiments 1 and 3 where
108 ACE2 was included in the screening library, we selected B cells with high LIBRA-seq scores for
109 S and low scores for ACE2; and for experiment 2, we selected B cells that had positive scores
110 for multiple aliquots of S (**Figure 1B-D**). B cells with high S and high ACE2 LIBRA-seq scores
111 were also selected as controls from experiments 1 and 3, along with an influenza-specific B cell
112 from experiment 2 (**Figure 1B-D**). Although some of the selected antibodies appeared to be
113 clonally related, overall they exhibited diverse sequence features, including V_H- and J_H-gene
114 usage, HCDR3 lengths, and somatic mutation numbers for both the heavy and light chains
115 (**Supplementary Figure 2A**).

116 To confirm the predicted antigen specificity for the selected antibodies, we tested them
117 for binding to S ectodomain by ELISA (**Figure 2A, Supplementary Figure 2B**). The LIBRA-seq
118 predicted antigen specificity was confirmed for 26 of 27 (96%) antibodies, including 25 SARS-
119 CoV-2 antibodies and 1 influenza virus antibody. Next, to map the general antibody epitope
120 regions, we also tested the antibodies for binding to S1, S2, receptor-binding domain (RBD),
121 and N-terminal domain (NTD) proteins (**Figure 2A, Supplementary Figure 2B**). The majority of
122 the antibodies from experiments 1 and 3 recognized the RBD, whereas none of the antibodies

123 from experiment 2 recognized the RBD, suggesting that the inclusion of a sequencing readout
124 for ACE2 blocking impacted the ability to select antibodies with target epitope specificities
125 (**Figure 2A, Supplementary Figure 2B**). The antibodies had a wide range of affinities for RBD
126 or NTD, including several ultra-potent antibodies (K_D <1 nM) from experiments 1 and 3 (**Figure**
127 **2B**). Next, we tested the ability of the antibodies to block ACE2 binding to spike. For the
128 antibodies predicted to block ACE2 by LIBRA-seq, 57% from experiment 1 and 67% from
129 experiment 3 demonstrated ACE2 blocking ability via ELISA (**Figure 2C, Supplementary**
130 **Figure 2C**). In contrast, no antibodies from experiment 2 blocked ACE2 binding (**Figure 2C,**
131 **Supplementary Figure 2C**). In addition, we tested the antibodies in a VSV SARS-CoV-2
132 chimeric virus neutralization assay. For the antibodies predicted to block ACE2 by LIBRA-seq,
133 86% from experiment 1 and 67% from experiment 3 were neutralizing (**Figure 2D-F**). In
134 contrast, only two clonally related antibodies (25%) from experiment 2 were neutralizing (**Figure**
135 **2D-F, Supplementary Figure 2D**). These results highlight the importance of including ligand
136 blocking in the LIBRA-seq screening for selectively identifying potently neutralizing antibodies.
137 Significant differences were not detected for the neutralization potencies between antibodies
138 from experiments 1 and 3 (p-value: >0.99, ANOVA with the Kruskal-Wallis Test; **Figure 2E**),
139 suggesting that antigen titrations did not have a significant effect on the ability to identify
140 potently neutralizing antibodies.
141 Next, we tested a panel of antibodies for neutralization of authentic SARS-CoV-2 virus in
142 a plaque reduction neutralization test and found that, just as in the VSV assay, antibody 5317-4
143 exhibited the most potent neutralization, with an IC_{50} value of 7.3 ng/mL (**Figure 2G**), on par
144 with antibodies currently in clinical trials or approved for emergency use[17-19]. In addition, to
145 investigate the recognition of SARS-CoV-2 S by LIBRA-seq-identified antibodies, we
146 determined a 9 Å-resolution Cryo-EM structure of the antigen-binding fragments (Fabs) of 5317-
147 4 and another neutralizing antibody, 5317-10, bound to the SARS-CoV-2 S extracellular domain
148 (ECD) (**Figure 2H**). We chose 5317-4 based on its potent neutralization, high affinity for the S

149 RBD, and ACE2 competition. The 3D reconstruction revealed that 5317-4 binds to the RBD in
150 the “up” and “down” conformations, and its epitope partially overlaps the ACE2 binding footprint
151 (**Figure 2H-I**). In the RBD up position, 5317-4 binds near the receptor-binding motif at an angle
152 that appears to moderately clash with RBD-bound ACE2 (**Figure 2I**). Additionally, when bound
153 to the RBD in the down conformation, 5317-4 competes with ACE2 binding to the adjacent,
154 otherwise accessible RBD in the up position (**Figure 2I**). 5317-10 was of interest due to its
155 inconclusive epitope bin, as it bound to S1, but not to the individual RBD or NTD constructs
156 (**Figure 2A**). The map revealed that 5317-10 binds a novel quaternary epitope that bridges an
157 RBD in the down position and the NTD of an adjacent protomer (**Figure 2H**). This mode of
158 recognition may prevent the RBD from transitioning into an ACE2-accessible up position,
159 thereby preventing binding by ACE2.

160 Together, the results from the three LIBRA-seq experiments showcase the advantages
161 of including ligand blocking as part of the sequencing readout. The experiment without ligand
162 blocking (experiment 2) had a lower hit rate for identifying virus-neutralizing antibodies. Through
163 a single high-throughput sequencing experiment, LIBRA-seq with ligand blocking identified ultra-
164 potent SARS-CoV-2 antibodies, requiring the subsequent production and validation of less than
165 a dozen antibodies per experiment. The observed hit rates for the discovery of potently
166 neutralizing antibodies are a substantial improvement over what has been reported in the
167 literature, which typically required the screening of hundreds to thousands of antibody
168 candidates to identify a small number of antibodies with similar levels of neutralization potencies
169 to the antibodies described in this manuscript[2-7]. The ability to save weeks or months during the
170 antibody lead discovery process can have an extraordinary impact on the evolution of an
171 infectious disease outbreak, especially in the early stages of infection spread. As such, the
172 application of LIBRA-seq with ligand blocking for the efficient discovery of highly potent
173 antibodies can provide critical advantages for rapid development of therapeutic and preventive
174 countermeasures. More broadly, LIBRA-seq with ligand blocking presents a general platform for

discovering functional antibodies, with applications to virtually any area where targeting the disruption of antigen-ligand interaction is a prime therapeutic goal.

Acknowledgements

We thank Angela Jones, Latha Raju, and Jamie Roberson of Vanderbilt Technologies for Advanced Genomics for their expertise regarding NGS and library preparation; David Flaherty and Brittany Matlock of the Vanderbilt Flow Cytometry Shared Resource for help with flow panel optimization; and members of the Georgiev laboratory for comments on the manuscript. The Vanderbilt VANTAGE Core provided technical assistance for this work. VANTAGE is supported in part by CTSA grant 5UL1 RR024975-03, the Vanderbilt Ingram Cancer Center (P30 CA68485), the Vanderbilt Vision Center (P30 EY08126), and NIH/NCRR (G20 RR030956). This work was conducted in part using the resources of the Advanced Computing Center for Research and Education at Vanderbilt University (Nashville, TN). Flow cytometry experiments were performed in the VUMC Flow Cytometry Shared Resource. The VUMC Flow Cytometry Shared Resource is supported by the Vanderbilt Ingram Cancer Center (P30 CA68485) and the Vanderbilt Digestive Disease Research Center (DK058404).

For work described in this manuscript, I.S.G., A.R.S., K.J.K., K.A.P., N.R., and L.W. were supported in part by NIH NIAID award R01AI131722-S1, the Hays Foundation COVID-19 Research Fund, Fast Grants, and CTSA award No. *UL1 TR002243* from the National Center for Advancing Translational Sciences. J.S.M, N.J., and D.W. were supported in part by a National Institutes of Health (NIH)/National Institute of Allergy and Infectious Diseases (NIAID) grant awarded to J.S.M. (R01-AI127521), Welch Foundation grant F-0003-19620604, and NIH NIAID award R01AI131722-S1. This work was supported by Defense Advanced Research Projects Agency (DARPA) grant HR0011-18-2-0001, U.S. N.I.H. contract 75N93019C00074, N.I.H. grant R01 AI157155, the Dolly Parton COVID-19 Research Fund at Vanderbilt, and a grant from Fast

Grants, Mercatus Center, George Mason University. J.E.C. is a recipient of the 2019 Future Insight Prize from Merck KGaA, which supported this work with a grant.

Author Contributions

Methodology, A.R.S., I.S., and I.S.G.; Investigation, A.R.S., N.J., K.J.K., N.S., D.W., S.P., K.A.P., N.J., R.N., R.E.S., L.W., J.E.C., A.B., R.H.C., J.S.M., and I.S.G.; Software, A.R.S., N.R.; Validation, A.R.S., K.J.K.; Writing - Original Draft, A.R.S. and I.S.G.; Writing -Review & Editing, all authors; Funding Acquisition, I.S.G., J.E.C., A.B., R.H.C., J.S.M., and A.R.S and K.J.K.; Resources, I.S.G., J.E.C., A.B., R.H.C., and J.S.M..; Supervision, I.S.G.

Declaration of Interest

A.R.S. and I.S.G. are co-founders of AbSeek Bio. I.S.G., A.R.S, and K.J.K. are listed as inventors on antibodies described herein. I.S.G., A.R.S, and I.S. are listed as inventors on patent applications for the LIBRA-seq technology. J.E.C. has served as a consultant for Luna Biologics, is a member of the Scientific Advisory Board Meissa Vaccines and is Founder of IDBiologics. The Crowe laboratory has received funding support in sponsored research agreements from AstraZeneca, IDBiologics, and Takeda. The Georgiev laboratory at Vanderbilt University Medical Center has received unrelated funding from Takeda Pharmaceuticals.

Data Availability Statement

All unique reagents generated in this study are available from the corresponding author with a completed Materials Transfer Agreement. Sequences for antibodies identified and characterized in this study will be deposited to GenBank and raw sequencing data will be deposited to Sequence Read Archive and will be available upon publication. Further information and requests for resources and reagents should be directed to the corresponding author, Ivelin Georgiev (Ivelin.Georgiev@Vanderbilt.edu).

226

227 **Code Availability**

228 Custom scripts used to analyze data in this manuscript are available upon request to the

229 corresponding author.

230

231 **METHODS**

232

233 **Donor Information**

234 PBMC samples were purchased from Cellero. The PBMCs were from subjects with past SARS-

235 CoV-2 infection at least 14 days post symptom cessation. For experiment 1, three samples were

236 pooled from donors 523, 527, and 528. For experiments 2 and 3, samples from donor 523 were

237 used for LIBRA-seq. Donor 523 had a plaque reduction neutralization test titer of 1:2,560.

238

239 **Antigen Purification**

240 A variety of recombinant soluble protein antigens were used in the LIBRA-seq experiment and

241 other experimental assays.

242 Plasmids encoding residues 1–1208 of the SARS-CoV-2 spike with a mutated S1/S2

243 cleavage site, proline substitutions at positions 817, 892, 899, 942, 986 and 987, and a C-

244 terminal T4-fibritin trimerization motif, an 8x HisTag, and a TwinStrepTag (SARS-CoV-2 spike

245 HP); 1−615 of human ACE2 with a C-terminal HRV3C protease cleavage site, a TwinStrepTag

246 and an 8XhisTag (ACE2) were transiently transfected in Expi293F cells using polyethylenimine.

247 Transfected supernatants were harvested 5 days after expression and purified over a StrepTrap

248 column (Cytiva Life Sciences), as previously described. Both recombinant SARS-CoV-2 S HP

249 and ACE2 were further purified to homogeneity using a Superose6 Increase column (Cytiva Life

250 Sciences).

251 For the HIV-1 gp140 SOSIP variant from strain ZM197 (clade C) and hemagglutinin from
252 strain A/New Caledonia/20/99 (H1N1) (GenBank ACF41878), recombinant, soluble antigens
253 contained an AviTag and were expressed in Expi293F cells using polyethylenimine transfection
254 reagent and cultured. FreeStyle F17 expression medium supplemented with pluronic acid and
255 glutamine was used. The cells were cultured at 37°C with 8% CO_2 saturation and shaking. After
256 5-7 days, cultures were centrifuged and supernatant was filtered and run over an affinity column
257 of agarose-bound *Galanthus nivalis* lectin. The column was washed with PBS and antigens
258 were eluted with 30 mL of 1M methyl-a-D-mannopyranoside. Protein elutions were buffer
259 exchanged into PBS, concentrated, and run on a Superdex 200 Increase 10/300 GL Sizing
260 column on the AKTA FPLC system. Fractions corresponding to correctly folded protein were
261 collected, analyzed by SDS-PAGE and antigenicity was characterized by ELISA using known
262 monoclonal antibodies specific to each antigen. AviTagged antigens were biotinylated using
263 BirA biotin ligase (Avidity LLC).
264 SARS-CoV-2 S1, SARS-CoV-2 S2, SARS-CoV-2 RBD and SARS-CoV-2 NTD proteins
265 were purchased from the commercial vendor, Sino Biological.
266
267 **DNA-barcoding of Antigens**
268 We used oligos that possess 15 bp antigen barcode, a sequence capable of annealing to the
269 template switch oligo that is part of the 10X bead-delivered oligos and contain truncated TruSeq
270 small RNA read 1 sequences in the following structure: 5′-
271 CCTTGGCACCCGAGAATTCCANNNNNNNNNNNNNNCCCATATAAGA*A*A-3′, where Ns
272 represent the antigen barcode as previously described[15]. For each antigen, a unique DNA
273 barcode was directly conjugated to the antigen itself. In particular, 5′ amino-oligonucleotides
274 were conjugated directly to each antigen using the SoluLINK Protein-Oligonucleotide
275 Conjugation Kit (TriLink cat no. S-9011) according to manufacturer's instructions. Briefly, the

276 oligo and protein were desalted, and then the amino-oligo was modified with the 4FB
277 crosslinker, and the biotinylated antigen protein was modified with S-HyNic. Then, the 4FB-oligo
278 and the HyNic-antigen were mixed. This process causes a stable bond to form between the
279 protein and the oligonucleotide. The concentration of the antigen-oligo conjugates was
280 determined by a BCA assay, and the HyNic molar substitution ratio of the antigen-oligo
281 conjugates was analyzed using the NanoDrop according to the SoluLINK protocol guidelines.
282 AKTA FPLC was used to remove excess oligonucleotide from the protein-oligo conjugates,
283 which were also verified using SDS-PAGE with a silver stain. Antigen-oligo conjugates were
284 also used in flow cytometric titration experiments.
285
286 **Antigen-specific B Cell Sorting**
287 Cells were stained and mixed with DNA-barcoded antigens and other antibodies, and then
288 sorted using fluorescence activated cell sorting (FACS). First, cells were counted, and viability
289 was assessed using trypan blue. Then, cells were washed three times with DPBS
290 supplemented with 0.1% bovine serum albumin (BSA). Cells were resuspended in DPBS-BSA
291 and stained with cell markers including viability dye (Ghost Red 780), CD14-APC-Cy7, CD3-
292 FITC, CD19-BV711, and IgG-PE-Cy5. Additionally, antigen-oligo conjugates were added to the
293 stain. After staining in the dark for 30 minutes at room temperature, cells were washed three
294 times with DPBS-BSA at 300 x g for five minutes. Cells were then incubated for 15 minutes at
295 room temperature with Streptavidin-PE to label cells with bound antigen. Cells were washed
296 three times with DPBS-BSA, resuspended in DPBS, and sorted by FACS. Antigen positive cells
297 were bulk sorted and delivered to the Vanderbilt Technologies for Advanced Genomics
298 (VANTAGE) sequencing core at an appropriate target concentration for 10X Genomics library
299 preparation and subsequent sequencing. Flow cytometry data were analyzed using FlowJo.
300
301 **Sample Preparation, Library Preparation, and Sequencing**

302 Single-cell suspensions were loaded onto the Chromium Controller microfluidics device (10X
303 Genomics) and processed using the B-cell Single Cell V(D)J solution according to
304 manufacturer's suggestions for a target capture of 10,000-20,000 B cells, with minor
305 modifications to intercept, amplify and purify the antigen barcode libraries as previously
306 described[15].
307

308 **Sequence processing and bioinformatic analysis**

309 We used our previously described pipeline to use paired-end FASTQ files of oligo libraries as
310 input, process and annotate reads for cell barcode, UMI, and antigen barcode, and generate a
311 cell barcode - antigen barcode UMI count matrix[15, 16]. BCR contigs were processed using Cell
312 Ranger (10X Genomics) using GRCh38 as reference. Antigen barcode libraries were also
313 processed using Cell Ranger (10X Genomics). The overlapping cell barcodes between the two
314 libraries were used as the basis of the subsequent analysis. We removed cell barcodes that had
315 only non-functional heavy chain sequences as well as cells with multiple functional heavy chain
316 sequences and/or multiple functional light chain sequences, reasoning that these may be
317 multiplets. Additionally, we aligned the BCR contigs (filtered_contigs.fasta file output by Cell
318 Ranger, 10X Genomics) to IMGT reference genes using HighV-Quest[20]. The output of HighV-
319 Quest was parsed using ChangeO[21] and merged with an antigen barcode UMI count matrix.
320 Finally, we determined the LIBRA-seq score for each antigen in the library by calculating the
321 centered-log ratios (CLR) of each antigen UMI count for each cell as previously described[15].
322

323 **Antibody Expression and Purification**

324 For each antibody, variable genes were inserted into custom plasmids encoding the constant
325 region for the IgG1 heavy chain as well as respective lambda and kappa light chains (pTwist
326 CMV BetaGlobin WPRE Neo vector, Twist Bioscience). Antibodies were expressed in Expi293F
327 mammalian cells (Thermo Fisher Scientific) by co-transfecting heavy chain and light chain

328 expressing plasmids using polyethylenimine transfection reagent and cultured for 5 to 7 days.
329 Cells were maintained in FreeStyle F17 expression medium supplemented at final
330 concentrations of 0.1% Pluronic Acid F-68 and 20% 4 mM L-Glutamine. These cells were
331 cultured at 37°C with 8% CO_2 saturation and shaking. After transfection and 5-7 days of culture,
332 cell cultures were centrifuged and supernatant was 0.45 µm filtered with Nalgene Rapid Flow
333 Disposable Filter Units with PES membrane. Filtered supernatant was run over a column
334 containing Protein A agarose resin equilibrated with PBS. The column was washed with PBS,
335 and then antibodies were eluted with 100 mM Glycine HCl at 2.7 pH directly into a 1:10 volume
336 of 1M Tris-HCl pH 8.0. Eluted antibodies were buffer exchanged into PBS 3 times using Amicon
337 Ultra-centrifugal filter units and concentrated. Antibody plasmids were sequenced. If antibody
338 sequences did not match expected heavy or light chain, antibody was excluded from
339 downstream analysis.
340
341 **High-throughput Antibody Expression**
342 For high-throughput production of recombinant antibodies, approaches were used that are
343 designated as microscale. For antibody expression, microscale transfection was performed
344 (~1 mL per antibody) of CHO cell cultures using the Gibco ExpiCHO Expression System and a
345 protocol for deep 96-well blocks (Thermo Fisher Scientific). In brief, synthesized antibody-
346 encoding DNA (~2 µg per transfection) was added to OptiPro serum free medium (OptiPro
347 SFM), incubated with ExpiFectamine CHO Reagent and added to 800 µL of ExpiCHO cell
348 cultures into 96-deep-well blocks using a ViaFlo 384 liquid handler (Integra Biosciences). The
349 plates were incubated on an orbital shaker at 1,000 r.p.m. with an orbital diameter of 3 mm at
350 37°C in 8% CO_2. The next day after transfection, ExpiFectamine CHO Enhancer and ExpiCHO
351 Feed reagents (Thermo Fisher Scientific) were added to the cells, followed by 4 d incubation for
352 a total of 5 d at 37°C in 8% CO_2. Culture supernatants were collected after centrifuging the

353 blocks at 450 x *g* for 5 min and were stored at 4°C until use. For high-throughput microscale
354 antibody purification, fritted deep-well plates were used containing 25 µL of settled protein G
355 resin (GE Healthcare Life Sciences) per well. Clarified culture supernatants were incubated with
356 protein G resin for antibody capturing, washed with PBS using a 96-well plate manifold base
357 (Qiagen) connected to the vacuum and eluted into 96-well PCR plates using 86 µL of 0.1 M
358 glycine-HCL buffer pH 2.7. After neutralization with 14 µL of 1 M Tris-HCl pH 8.0, purified
359 antibodies were buffer-exchanged into PBS using Zeba Spin Desalting Plates (Thermo Fisher
360 Scientific) and stored at 4°C until use.
361
362 **ELISA**
363 To assess antibody binding, soluble protein was plated at 2 µg/mL overnight at 4°C. The next
364 day, plates were washed three times with PBS supplemented with 0.05% Tween-20 (PBS-T)
365 and coated with 5% milk powder in PBS-T. Plates were incubated for one hour at room
366 temperature and then washed three times with PBS-T. Primary antibodies were diluted in 1%
367 milk in PBS-T, starting at 10 µg/mL with a serial 1:5 dilution and then added to the plate. The
368 plates were incubated at room temperature for one hour and then washed three times in PBS-T.
369 The secondary antibody, goat anti-human IgG conjugated to peroxidase, was added at 1:10,000
370 dilution in 1% milk in PBS-T to the plates, which were incubated for one hour at room
371 temperature. Plates were washed three times with PBS-T and then developed by adding TMB
372 substrate to each well. The plates were incubated at room temperature for ten minutes, and
373 then 1N sulfuric acid was added to stop the reaction. Plates were read at 450 nm.
374 Data are represented as mean ± SEM for one ELISA experiment. ELISAs were repeated 2 or
375 more times. If ELISA replicates were inconsistent over more than three experiments, antibody
376 was excluded from in vitro characterization analysis. The area under the curve (AUC) was
377 calculated using Prism software version 8.0.0 (GraphPad).
378

379 **ACE2 Binding Inhibition Assay**

380 96-well plates were coated with 2 µg/mL purified recombinant SARS-CoV-2 at 4°C overnight.
381 The next day, plates were washed three times with PBS supplemented with 0.05% Tween-20
382 (PBS-T) and coated with 5% milk powder in PBS-T. Plates were incubated for one hour at room
383 temperature and then washed three times with PBS-T. Purified anti were diluted in blocking
384 buffer at 10 µg/mL in triplicate, added to the wells, and incubated at room temperature. Without
385 washing, recombinant human ACE2 protein with a mouse Fc tag was added to wells for a final
386 0.4 µg/mL concentration of ACE2 and incubated for 40 minutes at room temperature. Plates
387 were washed three times with PBS-T, and bound ACE2 was detected using HRP-conjugated
388 anti-mouse Fc antibody and TMB substrate. The plates were incubated at room temperature for
389 ten minutes, and then 1N sulfuric acid was added to stop the reaction. Plates were read at 450
390 nm. ACE2 binding without antibody served as a control. Experiment was done in biological
391 replicate and technical triplicates.

392

393 **BioLayer Interferometry (BLI)**

394 Purified antibodies were immobilized to AHC sensortips (FortéBio) to a response level of
395 approximately 1.4 nm in a buffer composed of 10 mM HEPES pH 7.5, 150 mM NaCl, 3 mM
396 EDTA, 0.05% Tween 20 and 0.1% (w/v) BSA. Immobilized antibodies were then dipped into
397 wells containing two-fold dilutions of either SARS-CoV-2 RBD-SD1 (residues 306–577) or
398 SARS-CoV-2 NTD, ranging in concentration from 10–0.156 nM, to measure association
399 kinetics. Dissociation kinetics were measured by dipping sensortips into wells containing only
400 buffer. Data were reference subtracted and kinetics were calculated in Octet Data Analysis
401 software v10.0 using a 1:1 binding model.

402

403 **RTCA Method for Initial Screening of Antibody Neutralizing Activity**

404 To screen for neutralizing activity in the panel of recombinantly expressed antibodies, we used a
405 high-throughput and quantitative RTCA assay and xCelligence RTCA HT Analyzer (ACEA
406 Biosciences) that assesses kinetic changes in cell physiology, including virus-induced
407 cytopathic effect (CPE). Twenty µL of cell culture medium (DMEM supplemented with 2% FBS)
408 was added to each well of a 384-well E-plate using a ViaFlo384 liquid handler (Integra
409 Biosciences) to obtain background reading. Six thousand (6,000) Vero-furin cells in 20 µL of cell
410 culture medium were seeded per well, and the plate was placed on the analyzer. Sensograms
411 were visualized using RTCA HT software version 1.0.1 (ACEA Biosciences). For a screening
412 neutralization assay, equal amounts of virus were mixed with micro-scale purified antibodies in
413 a total volume of 40 µL using DMEM supplemented with 2% FBS as a diluent and incubated for
414 1 h at 37°C in 5% CO_2. At ~17–20 h after seeding the cells, the virus–antibody mixtures were
415 added to the cells in 384-well E-plates. Wells containing virus only (in the absence of antibody)
416 and wells containing only Vero cells in medium were included as controls. Plates were
417 measured every 8–12 h for 48–72 h to assess virus neutralization. Micro-scale antibodies were
418 assessed in four 5-fold dilutions (starting from a 1:20 sample dilution), and their concentrations
419 were not normalized. Neutralization was calculated as the percent of maximal cell index in
420 control wells without virus minus cell index in control (virus-only) wells that exhibited maximal
421 CPE at 40–48 h after applying virus–antibody mixture to the cells. An antibody was classified as
422 fully neutralizing if it completely inhibited SARS-CoV-2-induced CPE at the highest tested
423 concentration, while an antibody was classified as partially neutralizing if it delayed but did not
424 fully prevent CPE at the highest tested concentration[2, 22].
425
426 **Real-time Cell Analysis (RTCA) Neutralization Assay**
427 To determine neutralizing activity of IgG, we used real-time cell analysis (RTCA) assay on an
428 xCELLigence RTCA MP Analyzer (ACEA Biosciences Inc.) that measures virus-
429 induced cytopathic effect (CPE)[23]. Briefly, 50 µL of cell culture medium (DMEM supplemented

430 with 2% FBS) was added to each well of a 96-well E-plate using a ViaFlo384 liquid handler
431 (Integra Biosciences) to obtain background reading. A suspension of 18,000 Vero-E6 cells in
432 50 µL of cell culture medium was seeded in each well, and the plate was placed on the
433 analyzer. Measurements were taken automatically every 15 min, and the sensograms were
434 visualized using RTCA software version 2.1.0 (ACEA Biosciences Inc). VSV-SARS-CoV-2 (0.01
435 MOI, ~120 PFU per well) was mixed 1:1 with a dilution of antibody in a total volume of 100 µL
436 using DMEM supplemented with 2% FBS as a diluent and incubated for 1 h at 37°C in 5% CO_2.
437 At 16 h after seeding the cells, the virus-antibody mixtures were added in replicates to the cells
438 in 96-well E-plates. Triplicate wells containing virus only (maximal CPE in the absence of
439 antibody) and wells containing only Vero cells in medium (no-CPE wells) were included as
440 controls. Plates were measured continuously (every 15 min) for 48 h to assess virus
441 neutralization. Normalized cellular index (CI) values at the endpoint (48 h after incubation with
442 the virus) were determined using the RTCA software version 2.1.0 (ACEA Biosciences Inc.).
443 Results are expressed as percent neutralization in a presence of respective antibody relative to
444 control wells with no CPE minus CI values from control wells with maximum CPE. RTCA
445 IC_{50} values were determined by nonlinear regression analysis using Prism software.
446
447 **Plaque Reduction Neutralization Test (PRNT)**
448 The virus neutralization with live authentic SARS-CoV-2 virus (USA-WA1) was performed in the
449 BSL-3 facility of the Galveston National Laboratory using Vero E6 cells (ATCC CRL-1586)
450 following the standard procedure. Vero E6 cells were cultured in 96-well plates (10^4 cells/well).
451 Next day, 4-fold serial dilutions of antibodies were made using MEM-2% FBS, as to get an initial
452 concentration of 100 µg/mL. Equal volume of diluted antibodies (60 µL) were mixed gently with
453 original SARS-CoV-2 (USA-WA1) (60 µL containing 200 pfu) and incubated for 1 h at 37°C/5%
454 CO_2 atmosphere. The virus-serum mixture (100 µL) was added to cell monolayer in duplicates
455 and incubated for 1 at h 37°C/5% CO_2 atmosphere. Later, the virus-serum mixture was

456 discarded gently, and cell monolayer was overlaid with 0.6% methylcellulose and incubated for
457 2 days. The overlay was removed, and the plates were fixed in 4% paraformaldehyde twice
458 following BSL-3 protocol. The plates were stained with 1% crystal violet and virus-induced
459 plaques were counted. The percent neutralization and/or NT_{50} of antibody was calculated by
460 dividing the plaques counted at each dilution with plaques of virus-only control. For antibodies,
461 the inhibitory concentration at 50% (IC_{50}) values were calculated in Prism software (GraphPad)
462 by plotting the midway point between the upper and lower plateaus of the neutralization curve
463 among dilutions.
464
465 **Fab Preparation**
466 To generate Fabs, IgGs were incubated with Lys-C at 1:4,000 (weight:weight) overnight at
467 37 °C. EDTA free protease inhibitor (Roche) was dissolved to 25X and then added to the
468 sample at a final 1X concentration. The sample was passed over a Protein A column. The flow-
469 through was collected run on a Superdex 200 Increase 10/300 GL Sizing column on the AKTA
470 FPLC system. Fabs were visualized on SDS-PAGE.
471
472 **Electron Microscopy Sample Preparation and Data Collection**
473 Purified SARS-CoV-2 S HexaPro ectodomain[24] and Fabs 5317-4 and 5317-10 were combined
474 at a final complex concentration of 0.4 mg/mL. Fab 5317-10 was added to spike and incubated
475 on ice for 30 minutes before the addition of Fab 5317-4 immediately prior to grid deposition and
476 freezing. The complex was deposited on Au-300 1.2/1.3 grids that had been plasma cleaned for
477 4 minutes in a Solarus 950 plasma cleaner (Gatan) with a 4:1 ratio of O_2/H_2. Excess liquid was
478 blotted for 3 seconds with a force of -4 using a Vitrobot Mark IV (Thermo Fisher) and plunge
479 frozen into liquid ethane. 2,655 micrographs were collected from a single grid with the stage at a
480 30° tilt using a Titan Krios (Thermo Fisher) equipped with a K3 detector (Gatan). Movies were

481 collected using SerialEM[25] at 29,000X magnification with a corresponding calibrated pixel size
482 of 0.81 Å/ pixel.
483
484 **Cryogenic Electron Microscopy (Cryo-EM)**
485 Motion correction, CTF estimation, particle picking, and 2D classification were performed using
486 cryoSPARC v3.2.0[26]. The final iteration of 2D class averaging distributed 17,710 particles into
487 50 classes using an uncertainty factor of 3. From that, 13,232 particles were selected and an ab
488 inito reconstruction was performed with four classes followed by heterogeneous refinement of
489 those four classes. 6,803 particles from the highest-quality class were used for homogenous
490 refinement of the best volume without imposed symmetry. The resulting volume was used for an
491 additional round of homogenous refinement. To filter out additional junk particles, an *ab initio*
492 reconstruction was performed with three classes followed by heterogeneous refinement of those
493 three classes. 5,171 particles from the highest-quality class were used for homogenous
494 refinement of the best volume without imposed symmetry, resulting in a final 9 Å map.
495
496 **QUANTIFICATION AND STATISTICAL ANALYSIS**
497 ELISA error bars (standard error of the mean) were calculated using GraphPad Prism version
498 8.0.0. ANOVA analysis was performed for neutralization potency comparisons using GraphPad
499 Prism version 8.0.0.
500
501

502 **FIGURE CAPTIONS**

503

504 **Figure 1. Recovery of antibodies using LIBRA-seq with ligand blocking. A.** Experimental
505 setup of three LIBRA-seq experiments: experiment 1, LIBRA-seq with ligand blocking;
506 experiment 2, LIBRA-seq with a SARS-CoV-2 S titration; and experiment 3, LIBRA-seq with a
507 SARS-CoV-2 S titration and ligand blocking. After next-generation sequencing, hundreds of B
508 cells were recovered that had paired heavy/light chain sequencing information and antigen
509 reactivity information for the three experiments. For experiment 1 (**B**), 2 (**C**), and 3 (**D**), LIBRA-
510 seq scores for all cells per experiment are shown as open circles (n=828, 829, 957,
511 respectively). Antibodies chosen for expression and validation are highlighted in light blue.
512 LIBRA-seq scores for antigens in each experimental library for antibodies expressed are shown
513 from -2 to 2, as tan to purple, respectively. Scores outside of this range are shown as the
514 minimum and maximum values. For experiment 2 and 3, six different aliquots of S protein were
515 added in a titration series (1-6).

516

517 **Figure 2. Validation and characterization of expressed antibodies.** Names of antibodies
518 that were expressed and their characteristics are shown. Each row represents an antibody. **A.**
519 ELISA area under the curve (AUC) values for binding to SARS-CoV-2 recombinant antigen
520 proteins and a negative control influenza hemagglutinin protein are shown for antibodies in each
521 experiment calculated from data in Supplementary Figure 2B. **B.** Affinity (K_D) of antibodies for
522 SARS-CoV-2 RBD or NTD (based on epitope shown in A) was determined by biolayer
523 interferometry. ND, not done. **C.** Percent reduction in ACE2 binding by ELISA is shown as a
524 heatmap from 0 to 100% reduction in binding as white to blue respectively. **D.** VSV SARS-CoV-
525 2 neutralization IC_{50} values are shown as a heatmap from high potency (red) to low potency
526 (green). Non-neutralizing antibodies are shown as white. For **E** and **F**, "Predicted Neutralizing
527 Antibodies" were defined as the subset of selected antibodies with low ACE2 LIBRA-seq scores

528 from experiments 1 (7 antibodies) and 3 (6 antibodies), and all antibodies with high LIBRA-seq
529 scores for SARS-CoV-2 S from experiment 2 (7 antibodies). **E.** For these predicted neutralizers,
530 plotted are the IC_{50} values (µg/mL) for SARS-CoV-2 neutralization by real time cell analysis
531 (RTCA) with VSV-SARS-CoV-2 (IC_{50} value for each antibody shown as single dot). Line shown
532 is geometric mean. Non-neutralizing antibodies are shown as >10 µg/mL. **F.** The percent of
533 neutralizing antibodies from the set of predicted neutralizers is shown for each experiment. **G.**
534 Authentic SARS-CoV-2 neutralization for a panel of antibodies is shown. Data are represented as
535 mean ± SD. IC_{50} values are shown to the right of the panel. **H.** 10 Å-resolution cryo-EM structure
536 of Fab-spike complex for 5317-4 Fab (orange) and 5317-10 Fab (pink). Spike protomers are
537 shown in green, blue, and red. **I.** Fab-spike complex structure modeled with ACE2 (purple).
538
539 **Supplementary Figure 1. Set up of LIBRA-seq experiments.**
540 **A.** An antigen screening library of oligonucleotide-labeled antigens was generated. This library
541 consisted of SARS-CoV-2 spike antigens and negative controls. Additionally, oligo-labeled
542 ACE2 (the SARS-CoV-2 spike host cell receptor) was included. The antigen screening library
543 was mixed with donor PBMCs. This approach allowed for assessment of B cell ligand blocking
544 functionality from the sequencing experiment. **B.** We applied an antigen screening library
545 containing an antigen titration with a goal of identifying high affinity antibodies from LIBRA-seq.
546 In this experiment, six different amounts of oligo-labeled SARS-CoV-2 S protein, each labeled
547 with a different barcode, were included in a screening library, with the hypothesis that antibodies
548 with high affinity for SARS-CoV-2 S would show reactivity (high LIBRA-seq score) even with the
549 S protein added in lower amounts. **C**. Schematic of LIBRA-seq with S titrations and ACE2
550 included for ligand blocking.
551
552 **Supplementary Figure 2. Characterization of LIBRA-seq identified antibodies.**

553 **A.** Genetic characteristics for monoclonal antibodies prioritized for expression and validation.
554 V_H, J_H, V_L, J_L inferred gene segment identity is shown at the nucleotide level. CDRH3 and
555 CDRL3 amino acid sequence and length are shown. **B.** ELISA binding of antibodies to SARS-
556 CoV-2 spike, SARS-CoV spike, SARS-CoV-2 RBD, SARS-CoV-2 NTD, SARS-CoV-2 S2 and
557 influenza virus H1 NC99. ELISAs were performed in technical duplicates and repeated at least
558 two times. Data are represented as mean ± SEM. **C**. ACE2 blocking ELISA. Antibodies were
559 added to spike and recombinant ACE2 was added and detected. Antibodies that block ACE2
560 binding show a reduction in absorbance compared to ACE2 binding without competitor (dotted
561 line). ELISAs were performed at one antibody concentration in triplicate and were repeated at
562 least twice. Data are represented as mean ± SEM. **D.** Antibodies were tested in a VSV SARS-
563 CoV-2 RTCA neutralization assay. Neutralization curves and IC_{50} values are shown. Data are
564 represented as mean ± SD.
565

566 **References**

567 1. Jiang, S., Hillyer, C. & Du, L. Neutralizing Antibodies against SARS-CoV-2 and Other
568 Human Coronaviruses. *Trends Immunol* **41**, 355-359 (2020).
569 2. Zost, S.J. et al. Potently neutralizing and protective human antibodies against SARS-
570 CoV-2. *Nature* **584**, 443-449 (2020).
571 3. Chi, X. et al. A neutralizing human antibody binds to the N-terminal domain of the Spike
572 protein of SARS-CoV-2. *Science* **369**, 650-655 (2020).
573 4. Wec, A.Z. et al. Broad neutralization of SARS-related viruses by human monoclonal
574 antibodies. *Science* **369**, 731-736 (2020).
575 5. Brouwer, P.J.M. et al. Potent neutralizing antibodies from COVID-19 patients define
576 multiple targets of vulnerability. *Science* **369**, 643-650 (2020).

577 6. Rogers, T.F. et al. Isolation of potent SARS-CoV-2 neutralizing antibodies and protection
578 from disease in a small animal model. *Science* **369**, 956-963 (2020).
579 7. Hansen, J. et al. Studies in humanized mice and convalescent humans yield a SARS-
580 CoV-2 antibody cocktail. *Science* **369**, 1010-1014 (2020).
581 8. Krammer, F. SARS-CoV-2 vaccines in development. *Nature* **586**, 516-527 (2020).
582 9. Crowe, J.E., Jr. Principles of Broad and Potent Antiviral Human Antibodies: Insights for
583 Vaccine Design. *Cell Host Microbe* **22**, 193-206 (2017).
584 10. Scheid, J.F. et al. Broad diversity of neutralizing antibodies isolated from memory B cells
585 in HIV-infected individuals. *Nature* **458**, 636-640 (2009).
586 11. Wu, X. et al. Rational design of envelope identifies broadly neutralizing human
587 monoclonal antibodies to HIV-1. *Science* **329**, 856-861 (2010).
588 12. Busse, C.E., Czogiel, I., Braun, P., Arndt, P.F. & Wardemann, H. Single-cell based high-
589 throughput sequencing of full-length immunoglobulin heavy and light chain genes. *Eur J*
590 *Immunol* **44**, 597-603 (2014).
591 13. DeKosky, B.J. et al. High-throughput sequencing of the paired human immunoglobulin
592 heavy and light chain repertoire. *Nat Biotechnol* **31**, 166-169 (2013).
593 14. Tan, Y.C. et al. Barcode-enabled sequencing of plasmablast antibody repertoires in
594 rheumatoid arthritis. *Arthritis Rheumatol* **66**, 2706-2715 (2014).
595 15. Setliff, I. et al. High-Throughput Mapping of B Cell Receptor Sequences to Antigen
596 Specificity. *Cell* **179**, 1636-1646 e1615 (2019).
597 16. Shiakolas, A.R. et al. Cross-reactive coronavirus antibodies with diverse epitope
598 specificities and Fc effector functions. *Cell Rep Med*, 100313 (2021).
599 17. Chen, P. et al. SARS-CoV-2 Neutralizing Antibody LY-CoV555 in Outpatients with
600 Covid-19. *N Engl J Med* **384**, 229-237 (2021).
601 18. Cohen, M.S. Monoclonal Antibodies to Disrupt Progression of Early Covid-19 Infection.
602 *N Engl J Med* **384**, 289-291 (2021).

603 19. Weinreich, D.M. et al. REGN-COV2, a Neutralizing Antibody Cocktail, in Outpatients with
604 Covid-19. *N Engl J Med* **384**, 238-251 (2021).
605 20. Alamyar, E., Duroux, P., Lefranc, M.P. & Giudicelli, V. IMGT((R)) tools for the nucleotide
606 analysis of immunoglobulin (IG) and T cell receptor (TR) V-(D)-J repertoires,
607 polymorphisms, and IG mutations: IMGT/V-QUEST and IMGT/HighV-QUEST for NGS.
608 *Methods Mol Biol* **882**, 569-604 (2012).
609 21. Gupta, N.T. et al. Change-O: a toolkit for analyzing large-scale B cell immunoglobulin
610 repertoire sequencing data. *Bioinformatics* **31**, 3356-3358 (2015).
611 22. Gilchuk, P. et al. Integrated pipeline for the accelerated discovery of antiviral antibody
612 therapeutics. *Nat Biomed Eng* **4**, 1030-1043 (2020).
613 23. Suryadevara, N. et al. Neutralizing and protective human monoclonal antibodies
614 recognizing the N-terminal domain of the SARS-CoV-2 spike protein. *Cell* **184**, 2316-
615 2331 e2315 (2021).
616 24. Hsieh, C.L. et al. Structure-based design of prefusion-stabilized SARS-CoV-2 spikes.
617 *Science* **369**, 1501-1505 (2020).
618 25. Mastronarde, D.N. Automated electron microscope tomography using robust prediction
619 of specimen movements. *J Struct Biol* **152**, 36-51 (2005).
620 26. Punjani, A., Rubinstein, J.L., Fleet, D.J. & Brubaker, M.A. cryoSPARC: algorithms for
621 rapid unsupervised cryo-EM structure determination. *Nat Methods* **14**, 290-296 (2017).
622

Figure 1

A

Experiment 1: Ligand Blocking

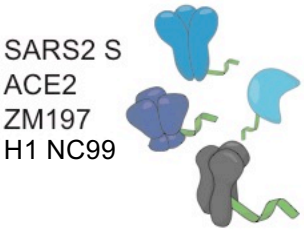

Experiment 2: SARS-CoV-2 S Titration

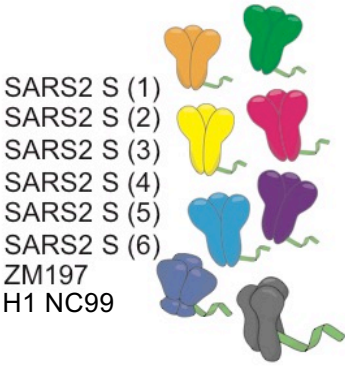

Experiment 3: SARS-CoV-2 S Titration + Ligand Blocking

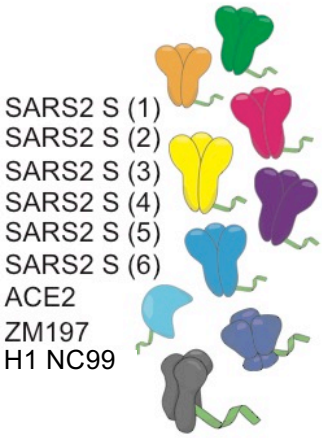

B

Experiment 1:Ligand Blocking

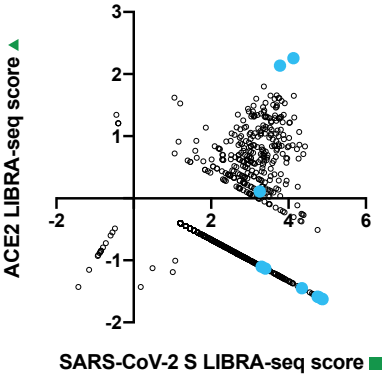

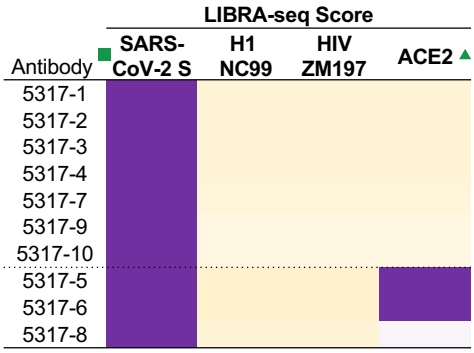

C

Experiment 2: SARS-CoV-2 S Titration

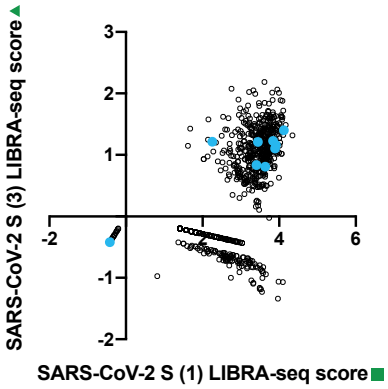

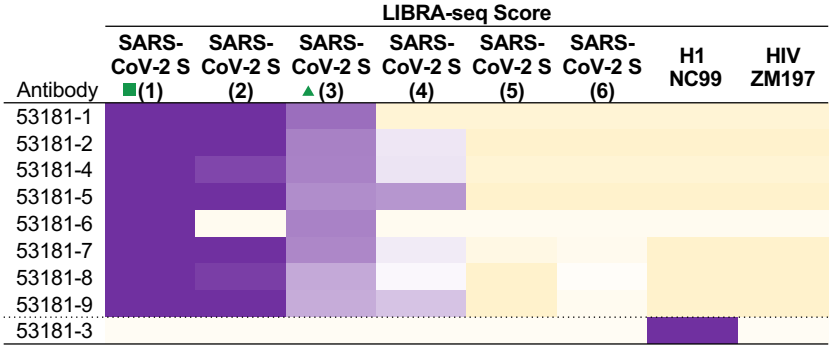

D

Experiment 3: SARS-CoV-2 S Titration + Ligand Blocking

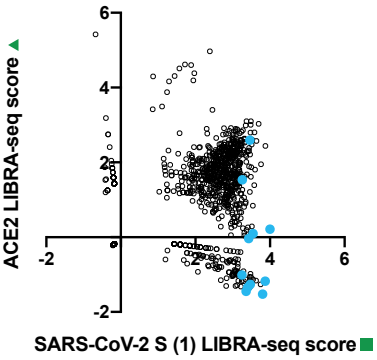

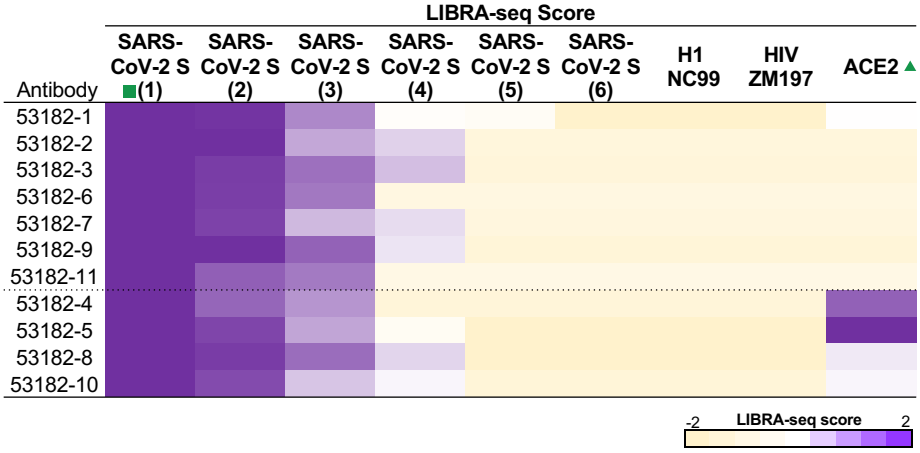

Figure 2

A

	Antibody	Binding Signal in ELISA (Area Under the Curve): SARS-CoV-2 S	SARS-CoV-2 S2	SARS-CoV-2 S1	SARS-CoV-2 RBD	SARS-CoV-2 NTD	H1 NC99	B: Affinity K_D (M)	C: % Reduction ACE2 Binding	D: Neut IC_{50} (µg/mL)
Experiment 1: Ligand Blocking	5317-1							4.34E-11	56	0.1218
	5317-2							1.95E-09	68	0.0829
	5317-3							1.92E-09	63	
	5317-4							1.78E-09	84	0.0148
	5317-7							1.05E-08	12	1.179
	5317-9							*ND*	-2	0.6326
	5317-10							*ND*	1	0.1816
	5317-5							8.26E-11	-3	
	5317-6							1.66E-09	0	
	5317-8							*ND*	-1	
Experiment 2: S Titration	53181-1							1.17E-09	-2	0.456
	53181-2							3.13E-08	-3	0.78
	53181-4							*ND*	0	
	53181-5							*ND*	-2	
	53181-7							*ND*	-1	
	53181-8							*ND*	-1	
	53181-9							*ND*	0	
	53181-3							*ND*	-1	
Experiment 3: S Titration + Ligand Blocking	53182-1							2.81E-09	84	0.343
	53182-3							8.32E-09	87	0.253
	53182-6							9.35E-10	91	0.077
	53182-7							2.15E-07	3	
	53182-9							4.75E-11	82	0.289
	53182-11							3.18E-09	7	
	53182-4							2.28E-09	0	
	53182-5							*ND*	-2	
	53182-8							1.65E-08	84	

ELISA AUC: min – max

% Reduction in Binding: 0 – 100

IC_{50} (µg/mL): 0.001 – 1 – 10

Non-neutralizing

E

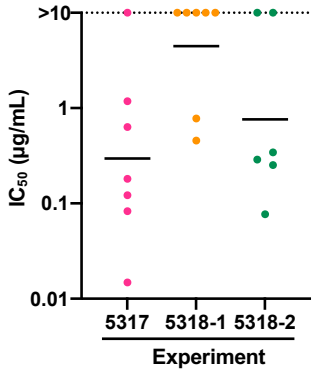

F

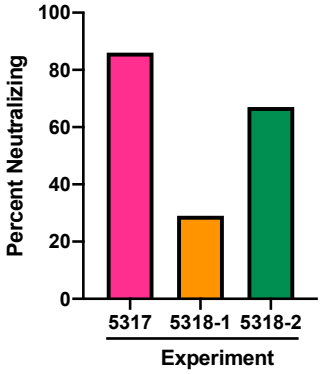

G

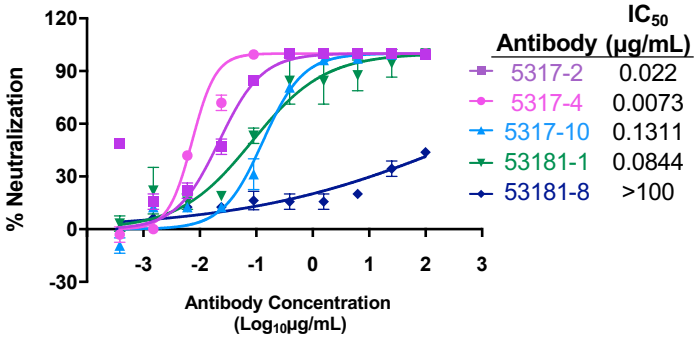

H

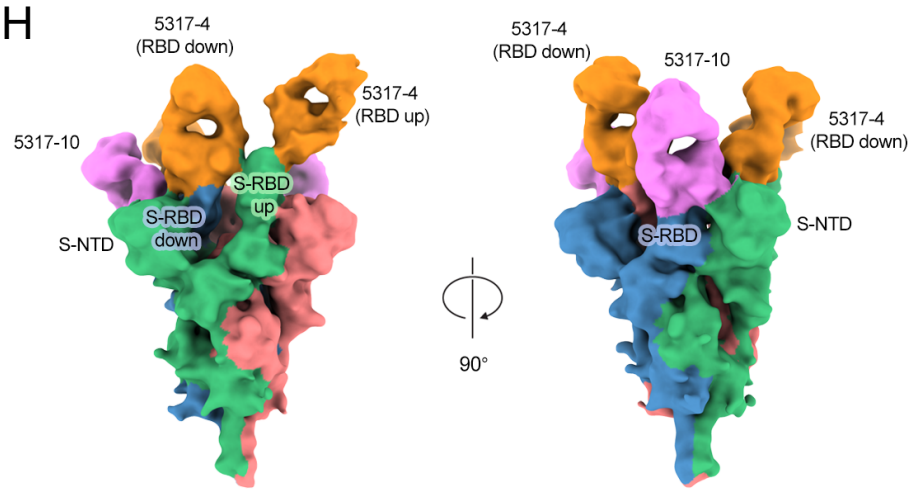

I

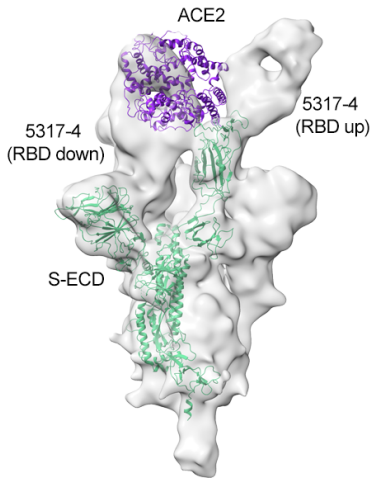

Supplementary Figure 1

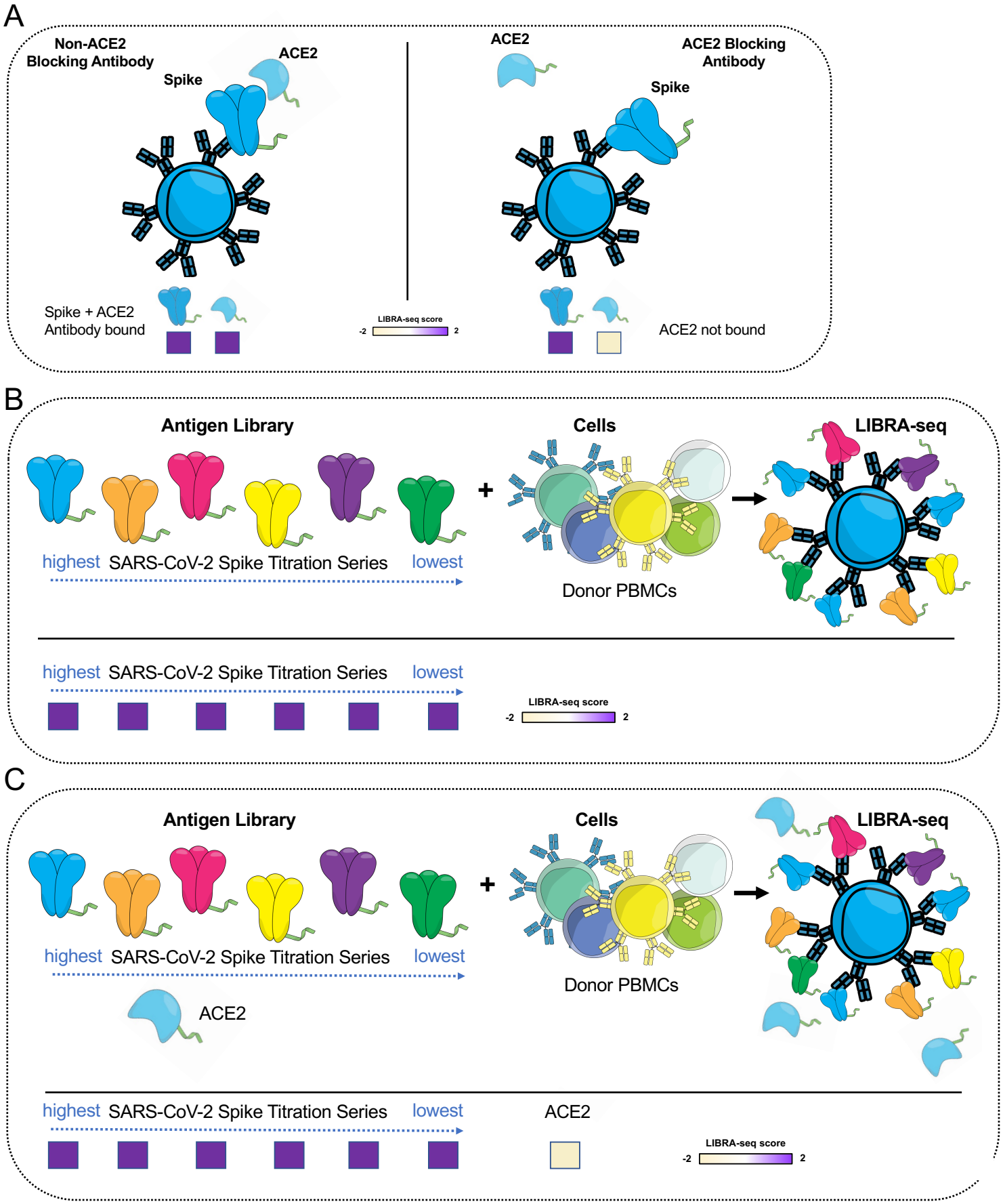

Supplementary Figure 2

A

Antibody	V^H Gene	J^H Gene	V^H Identity	J^H Identity	CDRH3 Sequence	CDRH3 Length	V^L Gene	J^L Gene	V^L Identity	J^L Identity	CDRL3 Sequence	CDRL3 Length
5317-1	*IGHV1-58*	*IGHJ4*	0.95	0.88	CAADPFADYW	8	*IGLV1-44*	*IGLJ3*	0.98	0.95	CATWDDSLNAWVF	11
5317-2	*IGHV1-69*	*IGHJ5*	0.95	0.92	CARGLWFGDSETVWFDPW	16	*IGKV1-39*	*IGKJ1*	0.97	0.97	CQQSYSTPPTF	9
5317-3	*IGHV3-64D*	*IGHJ4*	0.93	0.88	CVKGKIQLWLGADYW	13	*IGKV1-39*	*IGKJ1*	0.97	1.00	CQQSYNTPWTF	9
5317-4	*IGHV4-34*	*IGHJ3*	0.93	0.88	CARKPLLHSSVNPGAFDIW	17	*IGKV3-20*	*IGKJ2*	0.96	0.92	CQQYATSPRTF	9
5317-5	*IGHV1-69*	*IGHJ4*	0.97	0.96	CAREKGYSSSSSATYYLDFW	18	*IGLV1-40*	*IGLJ2*	0.98	0.95	CQSYDSSLTALVF	11
5317-6	*IGHV4-39*	*IGHJ6*	0.97	0.84	CARRVPGDYYCLDVW	13	*IGKV1-39*	*IGKJ4*	0.96	0.95	CQQSFSARVPTF	10
5317-7	*IGHV3-7*	*IGHJ4*	0.97	0.88	CARGGLWGTFDYW	11	*IGKV3-20*	*IGKJ2*	0.98	1.00	CQQFAYSLYTF	9
5317-8	*IGHV3-30-3*	*IGHJ6*	0.96	0.87	CARAYGGNYYYGMDVW	14	*IGLV3-1*	*IGLJ1*	0.96	0.97	CQAWDSSTASFVF	11
5317-9	*IGHV1-69*	*IGHJ5*	0.95	0.84	CASLGGDSYISGTHYDRSGYDPW	21	*IGKV3-11*	*IGKJ4*	0.98	0.95	CQRRSNWPPFTF	10
5317-10	*IGHV5-10-1*	*IGHJ4*	0.93	0.81	CARVNRVGDGPDFW	12	*IGKV2-28*	*IGKJ1*	0.97	1.00	CMQALQTPWTF	9
53181-1	*IGHV1-18*	*IGHJ6*	0.97	0.95	CARDPASYYDFWSGYVDYYYYGMDVW	24	*IGKV3-20*	*IGKJ3*	0.99	1.00	CQQYGNSRLTF	9
53181-2	*IGHV1-18*	*IGHJ6*	0.99	0.95	CARDPASYYDLWSGYVDYYYYGMDVW	24	*IGKV3-20*	*IGKJ3*	0.99	1.00	CHHYGSSRLTF	9
53181-3	*IGHV1-69*	*IGHJ4*	0.91	0.75	CARSGGYRLWFGELW	13	*IGKV3-20*	*IGKJ5*	0.94	0.95	CQQYGGSPATF	9
53181-4	*IGHV3-33*	*IGHJ4*	0.98	0.88	CAREGAVGATSGLDYW	14	*IGLV3-10*	*IGLJ3*	0.99	0.89	CYSRDSSGNPLF	10
53181-5	*IGHV4-59*	*IGHJ4*	0.95	0.96	CARGFDYW	6	*IGKV3-20*	*IGKJ1*	0.98	1.00	CQQYGSSPWTF	9
53181-6	*IGHV4-59*	*IGHJ6*	0.94	0.89	CARGAGEQRLVGGLFGVSHFYYYMDVW	25	*IGKV1-5*	*IGKJ1*	0.99	1.00	CQQYNSYPWTF	9
53181-7	*IGHV3-23*	*IGHJ4*	0.94	0.81	CAKSATIVLMVSAIYW	14	*IGLV2-14*	*IGLJ2*	0.97	1.00	CSSYTSTSTLVF	10
53181-8	*IGHV3-72*	*IGHJ6*	0.99	0.94	CARVRGGEWVGDLGWYYYYGMDVW	22	*IGKV2-28*	*IGKJ2*	0.99	0.97	CMQALQTPRTF	9
53181-9	*IGHV3-30*	*IGHJ4*	0.91	0.92	CVKGATKIDYW	9	*IGLV2-14*	*IGLJ1*	0.91	0.83	CFSYTSGGTRVF	10
53182-1	*IGHV3-53*	*IGHJ3*	0.95	0.96	CTRGGWPSGDTFDIW	13	*IGKV1-9*	*IGKJ3*	0.99	0.97	CQQLNSYPEITF	10
53182-2	*IGHV3-48*	*IGHJ5*	0.98	0.92	CAREGGWYSVGWVDPW	14	*IGKV3-20*	*IGKJ2*	0.98	0.97	CQQYGSSRTF	8
53182-3	*IGHV3-66*	*IGHJ6*	0.99	0.87	CARDRRIIGYYFGMDVW	15	*IGLV2-23*	*IGLJ3*	0.97	1.00	CCPYADTWVF	8
53182-4	*IGHV2-5*	*IGHJ3*	0.85	0.86	CARLLIEHDAFDIW	12	*IGKV2-28*	*IGKJ2*	0.92	0.97	CMQALHFPYTF	9
53182-5	*IGHV1-69*	*IGHJ4*	0.85	0.88	CAREEGSGWWKHDYW	13	*IGKV1-9*	*IGKJ2*	0.97	1.00	CQQLSGYPYTF	9
53182-6	*IGHV3-66*	*IGHJ6*	0.95	0.84	CVRDRRIVGYYFGLDVW	15	*IGLV2-23*	*IGLJ3*	0.96	0.95	CCSYATTWVF	8
53182-7	*IGHV3-23*	*IGHJ6*	0.98	0.97	CAKDAFYYGSGSHFYYYYYMDVW	21	*IGKV3-20*	*IGKJ5*	0.99	0.97	CQQYGSSPTF	8
53182-8	*IGHV4-39*	*IGHJ4*	0.99	0.92	CARDRRGGGWTASFDFW	15	*IGKV4-1*	*IGKJ2*	0.99	0.97	CQQHYSTPGYTF	10
53182-9	*IGHV3-53*	*IGHJ3*	0.98	0.98	CARGGWPSGDTFDIW	13	*IGKV1-9*	*IGKJ3*	0.99	0.97	CQQLNSYPEITF	10
53182-10	*IGHV2-5*	*IGHJ4*	0.98	0.83	CAHHTVPTIYDYW	11	*IGLV2-8*	*IGLJ3*	0.98	0.97	CSSYAGSNPLVF	10
53182-11	*IGHV3-9*	*IGHJ3*	0.93	0.92	CAKDIGRYDHYNIFGRVGGAFDIW	22	*IGKV1-33*	*IGKJ3*	0.95	0.94	CQHYDNLPRF	8

B

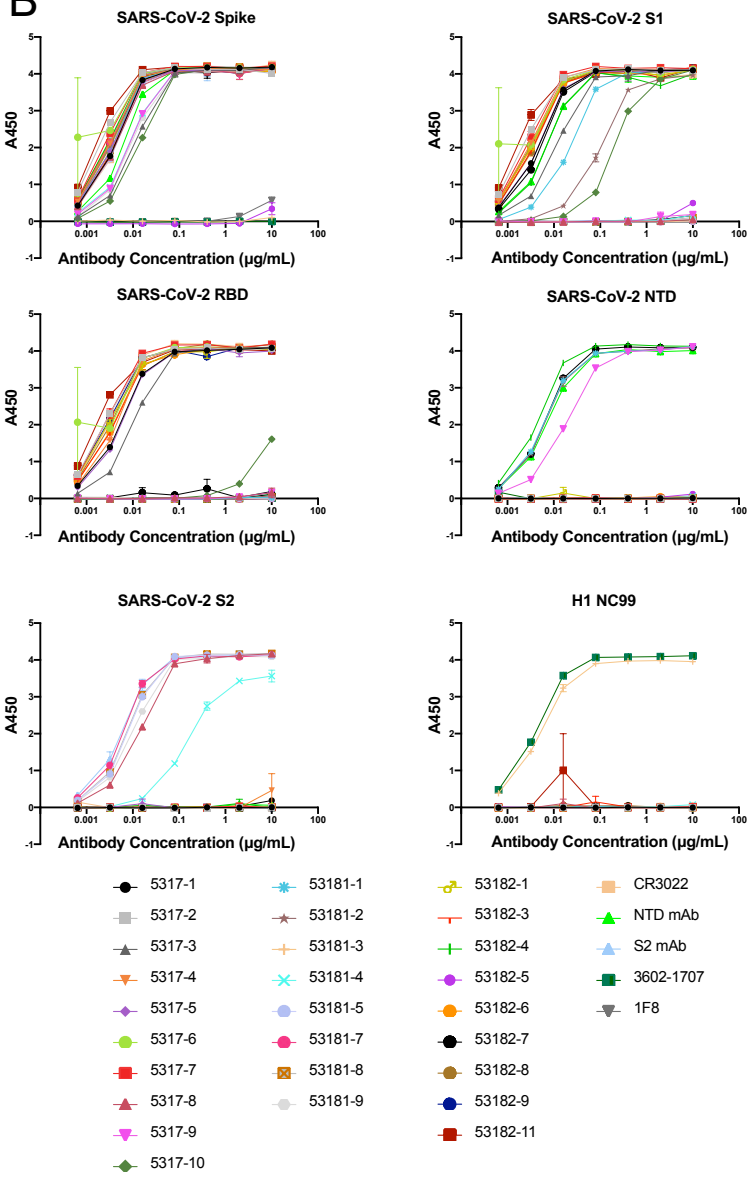

C

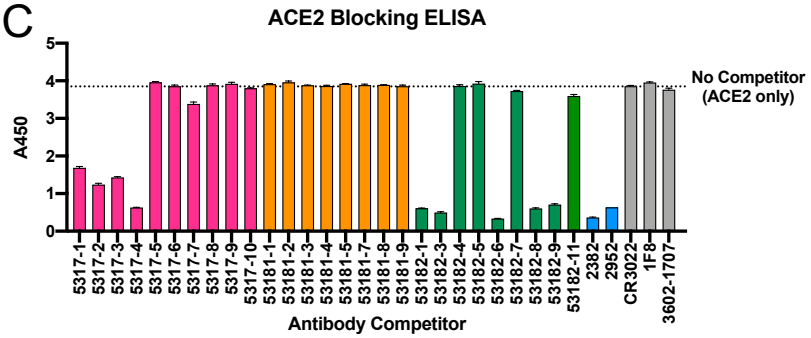
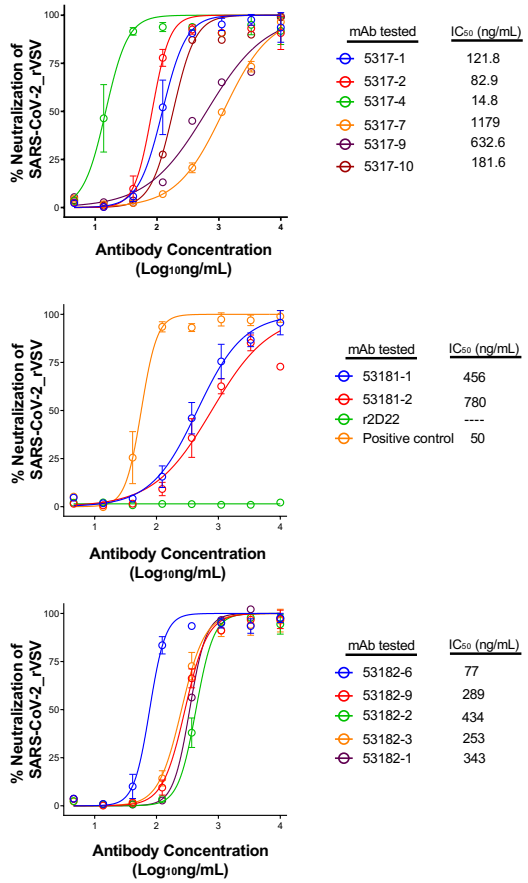
D